Carbohydrate Polymers 84 (2011) 907–918

Contents lists available at ScienceDirect

Carbohydrate Polymers

journal homepage: www.elsevier.com/locate/carbpol

Amylopectin internal molecular structure in relation to physical properties of sweetpotato starch

Fan Zhu [a,*], Harold Corke [a], Eric Bertoft [b]

[a] School of Biological Sciences, The University of Hong Kong, Pokfulam Road, Hong Kong, China
[b] Department of Food Science, Swedish University of Agricultural Sciences, P.O. Box 7051, S-750 07 Uppsala, Sweden

ARTICLE INFO

Article history:
Received 15 October 2010
Received in revised form
17 November 2010
Accepted 13 December 2010
Available online 21 December 2010

Keywords:
Internal unit chain distribution
Sweetpotato amylopectin structure
Chain category
Structure–properties relationship

ABSTRACT

Unit chain length distributions of amylopectins and their φ,β-limit dextrins (reflecting amylopectin internal part) from 11 Chinese sweetpotato genotypes were characterized by high performance anion-exchange chromatography after debranching, and were related to the thermal and pasting properties of granular starches. The weight-based unit chain length profiles of whole amylopectin and their internal parts both had three distinguishable major groups with approximate range of DP 6–36, 37–68, and >69 for amylopectins and DP 3–25, 26–55, and >55 for φ,β-limit dextrins. Among different genotypes, two different patterns of B_{fp} (fingerprint B-chains, DP 3–7) were observed for φ,β-limit dextrins, whereas A_{fp} (fingerprint A-chains, DP 6–8) for whole amylopectins were consistent. Reconstruction of amylopectins from their φ,β-limit dextrins revealed that B-chains with internal DP > 20 possessed an external chain length corresponding to the average value DP 12.8. Wide genetic variations were recorded among structural parameters, of which several concerning the amylopectin internal part were highly correlated to the thermal and pasting parameters of sweetpotato starches, and suggested that the internal part of amylopectin is critical to the physical behavior of granular starch.

1. Introduction

Amylopectin is a branched biomacromolecular component in starch and consists solely of D-glucose residues which are covalently interconnected mostly by α-(1 → 4) glucosidic but also about 5% α-(1 → 6) glucosidic bonds. Despite the simplicity in the chemical composition, the exact amylopectin structure remains largely unknown due to the technical limitations in chromatographic separation of amylopectin macromolecules, which have large range of molecular weight distributions (Buléon, Colonna, Planchot, & Ball, 1998). Nevertheless, the structure of amylopectin could be described in an average way by conceptually treating all the amylopectin macromolecules as a single type. Routine works usually include debranching isolated amylopectin by isoamylase and/or pullulanase, and then subjecting the linear hydrolysates to chromatographic analysis to obtain the unit chain length distribution of the whole amylopectin (Hizukuri, 1986). In this way, amylopectins from many diverse plants/genotypes have been characterized (Hanashiro, Abe, & Hizukuri, 1996; Jane et al., 1999; Sanderson, Daniels, Donald, Blennow, & Engelsen, 2006), and it has been established that the unit chain length profiles of amylopectins are highly related to physical behaviors and structures (e.g., X-ray diffraction pattern) of their respective granular starches (Hizukuri, 1985; Vermeylen, Goderis, Reynaers, & Delcour, 2004). It was shown that in general B-type starches had longer average amylopectin chain length than A-type starches, whereas C-type falls in between (Hizukuri, 1985; Jane et al., 1999).

Computational modeling showed that structures of internal chain segments are critical to the architecture of building blocks of amylopectins, and eventually the polymorph type of granular starch (O'Sullivan & Pérez, 1999). The amorphous regions in starch granules, which mostly consist of internal chain segments of amylopectin, can be highly influential to their physicochemical properties (e.g., thermal properties) (Donovan, 1979; Genkina, Wikman, Bertoft, & Yuryev, 2007; Slade & Levine, 1988; Waigh et al., 2000). By profiling the starch-water phase transitions in the presence of different amounts of water, Donovan (1979) proposed that the initial swelling of the amorphous regions of the granules with increasing thermal motion during hydration would pull the chains from the surfaces of crystallites, eventually resulting in full gelatinization of starch. By applying partial-heating and quench-cooling techniques to A-type cereal starches, Slade and Levine (1988) identified the non-equilibrium temperature locations of the effective glass transition and effective "end of melting" temperatures, and proposed on the basis

* Corresponding author. Tel.: +852 22990314; fax: +852 28583477.
E-mail address: fzhu5@yahoo.com (F. Zhu).

0144-8617/$ – see front matter.
doi:10.1016/j.carbpol.2010.12.039

of Williams–Landel–Ferry free volume theory that they were to a large extent dependent on the thermodynamic softening of the amorphous regions of granules during hydration. By small-angle X-ray scattering (SAXS), wide-angle X-ray scattering (WAXS), and cross-polarized magic-angle-spinning carbon-13 nuclear magnetic resonance spectroscopy (^{13}C CP/MAS NMR), granular starch was analogized to a chiral side-chain polymeric liquid crystal model to explain diverse physical behaviors of starch such as the phase transformations in starch during gelatinization and freezing (Waigh et al., 2000). The mesogens in the model of Waigh et al. (2000) apparently belonged to the crystallites, and the amorphous part of granules consisted of flexible backbones and spacers, which were essentially important to the physical behaviors of the whole liquid crystal. However, chemical evidence at molecular levels to support the above mentioned results, obtained by physical methods, remains to be established. The amorphous parts of the granules usually consist of the densely branched building blocks interconnected to form the internal part of amylopectins (Pérez & Bertoft, 2010). Amylopectin internal part can be experimentally isolated by exo-acting enzymes such as phosphorylase *a* and/or β-amylase to obtain the φ,β- or β-limit dextrins (Bertoft, 2004). In the form of φ,β-limit dextrins, all the A-chain (Peat, Whelan, & Thomas, 1952) would appear as maltose stubs, whereas the rest other than maltose stubs are B-chains (Bertoft, 2004). However, very limited number of internal structures of amylopectins from selected plants has been characterized and structurally related to the physicochemical properties of granular starches.

Sweetpotato (*Ipomoea batatas* (L.) Lam.) is one of the most important economic crops in many tropical and sub-tropical countries in Asia, Africa, and Latin America. Its adaptability on marginal land and its relatively rich nutritional content provide an enormous potential for preventing malnutrition and enhancing food security in the developing countries (Zhang, Ghislain, Huamán, Golmirzaie, & Hijmans, 1998). China is the largest sweetpotato producer accounting for 90% of global production (International Potato Center, 2010). Sweetpotato cultivation in China is distributed over a large biogeographic area and is abundant in genetic resources (Zhang, 2001). The major component of sweetpotato roots is starch, which usually has a C- or C_a-type polymorph (Tian, Rickard, & Blanshard, 1991). However, the diversity in starch quality and amylopectin structure from Chinese sweetpotato roots is little documented.

Previous studies on unit chain length compositions of internal part of different amylopectins in the form of φ,β-limit dextrins from some plant sources have been reported (Bertoft & Koch, 2000; Bertoft, Piyachomkwan, Chatakanonda, & Sriroth, 2008; Kong, Bertoft, Bao, & Corke, 2008; Laohaphatanaleart, Piyachomkwan, Sriroth, Santisopasri, & Bertoft, 2009). Based on the proportions of diverse internal B-chain categories, various amylopectins were tentatively classified into four structural groups 1–4 (Bertoft et al., 2008). Group 1 (e.g., oat) had the lowest amout of BL-chains (long B-chains, which includes B2- and B3-chains) and the highest amount of BS-chains (short B-chains, also named B1-chains). Group 2 (e.g., waxy maize) and group 3 (e.g., mung bean) contained intermediate amounts of B3-chains and group 2 had higher amounts of B_{fp} (fingerprint B-chains) compared with group 3. Group 4 (e.g., potato) contained the highest amount of BL-chains and the lowest amount of BS-chains. However, this classification remains to be confirmed. This study attempted to expand the previous structural collections to include amylopectins of 11 sweetpotato genotypes collected from different parts of China; and to correlate these structural parameters of the internal part of amylopectins to the thermal and pasting properties of sweetpotato starches.

2. Materials and methods

2.1. Materials

Sweetpotato roots of 11 genotypes with different geographic origins in China were kindly provided by Hubei Academy of Agricultural Sciences, Wuchang, Wuhan, Hubei Province, China. The background information of diverse genotypes is described in Table 1. For the province of origin, Yuzi263 was from Chongqing, Xuzi13-4 and Xushu22 were from Jiangsu, and the rest were from Hubei. They were grown at the Experimental Farm of the Institute of Crop Science, Hubei Academy of Agricultural Sciences, Wuhan, China, in the year 2008. The soil type of the experimental field was loam. The agronomic traits of sweetpotatoes were previously described (Zhu, Cai, Yang, Ke, & Corke, 2010). The isolation and purification of starch from sweetpotato roots generally followed a previous description (Collado, Mabesa, & Corke, 1999).

Rabbit muscle phosphorylase *a* (EC 2.4.1.1, 23 U/mg), was from Sigma–Aldrich, Deisenhofen, Germany. Barley β-amylase (EC 3.2.1.2, 620 U/mg), *Pseudomonas amyloderamosa* isoamylase (EC 3.2.1.68, 91 U/mg), and *Klebsiella planticola* pullulanase (EC 3.2.1.41, 36.3 U/mg) were from Megazyme International, Wicklow, Ireland. The given enzyme activities were according to the suppliers.

2.2. Production of amylopectin

Amylopectin fractionation was conducted following previous reports (Klucinec & Thompson, 1998; Kong et al., 2008) with some modifications. Granular starch (2.5 g) was dissolved in 90% dimethyl sulfoxide (DMSO) in water (50 mL) in a 250 mL Erlenmeyer flask sealed with aluminum foil. The flask containing the mixture was then heated in a boiling water bath with constant stirring on a magnetic stirrer with heated plate for 3 h, making sure that no gelatinous lumps remained. After dissolution of starch, the clear solution was placed at room temperature (24 °C) for 10 min whereafter 96% ethanol (200 mL) was slowly added with continuous stirring for 15 min to precipitate the dissolved starch. The slurry was centrifuged at 3000 × *g* for 10 min. The supernatant was discarded and the sediment was resuspended in 96% ethanol (50 mL) and then centrifuged at 3000 × *g* for 10 min. The washing procedure was performed once more using acetone (50 mL). The final precipitate was put in an air-forced oven at 45 °C for about 24 h and termed non-granular starch.

The non-granular starch (2.0 g) was dispersed in 90% DMSO (56 mL) by heating as above in a 500 mL Erlenmeyer flask. After cooling at room temperature for 15 min, solution of 6% 1-butanol and 6% isoamyl alcohol in water (400 mL) was added to the flask. The mixture was stirred on a magnetic stirrer for 15 min and placed in a 95 °C circulating water bath (W28, Grant, Barrington, England) for 1 h, and then the entire system was cooled to 28 °C for about 20 h. The mixture was stirred on a magnetic stirrer to resuspend any precipitation for 15 min and centrifuged for 15 min (10,000 × *g*, 4 °C). The supernatant was concentrated under vacuum to 100 mL at 60 °C using a rotary evaporator (R114 Rotovapor with a B480 water bath, Büchi, Switzerland). The concentrated fraction was precipitated by ethanol and washed by acetone with the same procedure as for the preparation of non-granular starch. The resultant precipitates were freeze-dried for about 24 h. The dried sample was fractionated amylopectin and sealed in plastic cups until use.

2.3. Analysis of amylopectin purity by gel permeation chromatography

Purified amylopectin (2.0 mg) was completely dissolved in 90% DMSO (50 μL) by heating for 15 min in boiling water bath with constant magnetic stirring. The solution was diluted by adding 400 μL

Table 1
Basic background information of 11 Chinese sweetpotato genotypes and weight- and molar-based unit chain length distribution of debranched amylopectins.[a]

Code	Name	Category	Weight-based unit chain length distribution (%)							Molar-based unit chain length distribution (%)						
			fa	fb1	fb2	fb3	fa/fb1	fa/fb1-2	fa/fb1-3	Fa	Fb1	Fb2	Fb3	Fa/Fb1	Fa/Fb1-2	Fa/Fb1-3
1	E6107b	Landrace	17.17^{ab}	42.02^{cd}	15.86^{ab}	24.96^{de}	0.41	0.30	0.21	35.34	45.32	10.35	9.00	0.78	0.64	0.55
2	E6107a	Breeding line	17.32^{ab}	41.91^{cd}	15.68^{ab}	25.10^{cd}	0.42	0.30	0.21	35.54	45.28	10.22	8.96	0.79	0.64	0.55
3	Yuzi263	Cultivar	17.08^{ab}	41.28^{cd}	15.95^{a}	25.71^{b}	0.41	0.30	0.21	35.53	44.75	10.46	9.26	0.80	0.64	0.55
4	Xuzi13-4	Cultivar	16.41^{bc}	43.49^{bc}	15.30^{bc}	24.81^{e}	0.38	0.28	0.20	33.60	47.33	10.07	9.01	0.71	0.59	0.51
5	E5306	Breeding line	17.43^{ab}	42.65^{cd}	15.33^{bc}	24.59^{de}	0.41	0.30	0.21	35.57	45.71	9.95	8.78	0.78	0.64	0.55
6	Eshu-6	Cultivar	16.71^{ab}	45.07^{a}	14.81^{d}	23.41^{f}	0.37	0.28	0.20	33.56	48.35	9.62	8.47	0.70	0.58	0.51
7	Ea2	Landrace	16.58^{bc}	41.86^{cd}	15.54^{bc}	26.03^{ab}	0.40	0.29	0.20	34.43	45.84	10.31	9.42	0.75	0.62	0.53
8	Ea3-1	Landrace	17.47^{a}	42.24^{cd}	15.44^{bc}	25.11^{cd}	0.42	0.31	0.21	35.76	45.43	9.86	8.96	0.79	0.65	0.56
9	Ea4	Landrace	16.95^{ab}	41.13^{d}	15.44^{bc}	26.49^{a}	0.41	0.30	0.20	35.32	44.99	10.22	9.47	0.79	0.64	0.55
10	Ea3-2	Breeding line	17.04^{ab}	42.27^{cd}	15.26^{cd}	25.44^{bc}	0.40	0.30	0.21	35.06	45.84	10.02	9.10	0.77	0.63	0.54
11	Xushu22	Cultivar	15.75^{c}	43.54^{bc}	15.12^{cd}	25.61^{b}	0.36	0.27	0.19	32.54	47.95	10.10	9.42	0.68	0.56	0.48
Mean	16.90	42.49	15.43	25.20	0.40	0.29	0.20	34.75	46.07	10.11	9.08	0.76	0.62	0.53		

"f" Denotes weight-based values, "F" denotes molar-based values. fa/fb1, fa/fb1-2, and fa/fb1-3 denote the ratios of percentages: fa/fb1, fa/(fb1 + fb2), and fa/(fb1 + fb2 + fb3), respectively; values in the same column with the different superscript letters differ significantly ($p < 0.05$), since weight-based unit chain length distribution and molar-based unit chain length distribution shared the same pattern in their difference in mean values, only the former were labeled.

[a] The range of DP (degree of polymerization) for different fractions: fa and Fa, DP 6–12; fb1 and Fb1, DP 13–24; fb2 and Fb2, DP 25–36; fb3 and Fb3, DP > 36.

warm water and 50 μL sodium acetate buffer (pH 5.5, 0.01 M). After cooling the diluted solution to room temperature (~23 °C), 1 μL isoamylase and 1 μL pullulanase were added. The debranching reaction was conducted with constant stirring at room temperature for 12 h at a concentration of 4.0 mg/mL, and then 50 μL NaOH (5 M) was added to inactivate the debranching enzymes. Sample (200 μL) was injected onto a column (1 cm × 90 cm) of Sepharose CL 6B (Pharmacia, Uppsala, Sweden). The eluent was sodium hydroxide in water (0.5 M) with a pumping speed of 0.5 mL/min. Collected fractions (0.5 mL) were analyzed for carbohydrate content by the phenol-sulphuric acid reagents (Dubois, Gilles, Hamilton, Rebers, & Smith, 1956). The column was calibrated with both linear and branched dextrins of known DP as previously described (Bertoft & Spoof, 1989).

2.4. Production of φ,β-limit dextrins

The production of φ,β-limit dextrins from amylopectins was performed according to a previous description with minor modifications (Laohaphatanaleart et al., 2009). The purified amylopectin (200 mg) was dissolved in 6 mL 90% DMSO by heating in boiling water bath for 15 min and then at room temperature for 12 h with constant magnetic stirring to completely dissolve the amylopectins. The solution was diluted by adding 65.4 mL warm double distilled water. Then 7.2 mL sodium phosphate buffer (pH 6.8, 1.1 M), 3.4 mL Na-EDTA (2.8 mM), and 18 mL freshly prepared rabbit muscle phosphorylase *a* solution (0.9 U/mL) were added and kept stirring for 12 h at room temperature. The substrate for phosphorolysis was 2 mg/mL. The reaction was terminated in a boiling water bath for 5 min. The α-D-glucose 1-phosphate produced and small ions were removed by tangential flow filtration with an Omega 10 K membrane in Minimate™ TFF Capsule System (Pall Life Sciences, Ann Arbor, MI, USA). This phosphorolysis was repeated once to obtain the φ-limit dextrins. The sample was concentrated by rotary evaporation, and then sodium acetate buffer (0.01 M, pH 6.0) (0.325 volume) and barley β-amylase (0.001 volume) were added to the φ-limit dextrins solution (1 volume). The substrate concentration was 5 mg/mL for β-amylolysis. The reaction was conducted for 12 h at room temperature with constant stirring, and terminated by boiling. Maltose was removed by membrane filtration as above. The β-amylolysis was repeated once and the φ,β-limit dextrins were freeze-dried.

2.5. High-performance anion-exchange chromatography of unit chain length profiles of amylopectins and φ,β-limit dextrins

Amylopectins or φ,β-limit dextrins (2.0 mg) were dissolved in 90% DMSO (50 μL) by heating for 15 min in boiling water bath with constant stirring on a magnetic stirrer. The solution was diluted by adding 400 μL warm water and 50 μL sodium acetate buffer (pH = 5.5). After cooling the diluted solution to room temperature (~23 °C), 1 μL isoamylase and 1 μL pullulanase were added. The debranching reaction was conducted with constant stirring at room temperature for 12 h at a substrate concentration of 4.0 mg/mL, and was then heated on boiling water bath for 1 min to inactivate the debranching enzymes. Double distilled water (1.5 mL) was added to dilute the sample to a concentration of 1.0 mg/mL. The debranched sample was filtered through a 0.45 μm syringe-driven filter unit before injecting into high-performance anion-exchange chromatography (HPAEC) system for unit chain length profile determination.

HPAEC system was a Dionex DX 500 instrument (Sunnyvale, CA, USA) consisted of a GP40 gradient pump, an ED 40 electrochemical detector for pulsed amperometric detection (PAD), and an autosampler (Spectra-Physics, Fremont, CA, USA). The PAD-signal was adjusted to carbohydrate content for quantification according to Koch, Andersson and Åman (1998). The analytical column was a CarboPac PA-100 anion-exchange column (4 mm × 250 mm), combined with a CarboPac PA-100 guard column (4 mm × 50 mm). The flow rate was 1.0 mL/min and injection volume was 20 μL. The mobile phases were eluent A (0.15 M NaOH) and eluent B (0.15 M NaOH containing 0.5 M NaOAc). A gradient elution (130 min) was used as follows: 0–9 min, 15–36% B; 9–18 min, 36–45% B; 18–110 min, 45–100% B; 100–112 min, 100–15% B; 112–130 min, 15% B.

2.6. Statistical analysis

All determinations were conducted in triplicate. The reported data and chromatograms were the mean values. Differences between means of data were compared by Fisher's least significant difference at significance level $p < 0.05$ and Pearson correlation analysis were conducted, using Statistical Analysis System (SAS Institute, Cary, NC).

3. Results and discussion

3.1. Unit chain length distributions of amylopectins

The purified amylopectins were analyzed on gel permeation chromatography after debranching to measure the purity. An example of comparison of purified amylopectins with whole starch from sweetpotato genotype 9 is shown in Fig. 1A. Fractions 45–77 were attributed to the amylose, whereas fractions 79–125 were considered to be amylopectin chains. In this study, all the isolated amylopectins were considered pure when the amylose remnant was below 3%.

The purified amylopectins were debranched and analyzed by HPAEC for the unit chain length distributions. The profiles, taking the chromatograms of genotype 6 and 8 as examples (Fig. 1B and C), generally agreed with previous descriptions (Hanashiro et al., 1996; Noda et al., 1998). According to Hanashiro et al. (1996), the unit chains were categorized into four fractions: fa ("f" for weight-based) or Fa ("F" for molar-based) with DP 6–12; fb1 or Fb1 with DP 13–24; fb2 or Fb2 with DP 25–36; fb3 or Fb3 with DP >36. Illustrations of the divisions of DP are shown in Fig. 1B. Quantitative results are presented in Table 1. Wide genetic variations were recorded among different proportions for different fractions from the debranched sweetpotato amylopectins. Genotype 11 had the lowest weight- and molar-based percentages of fraction fa, resulting in the lowest ratios of fa/fb1, fa/fb1-2, and fa/fb1-3, whereas genotype 8 had the highest percentage of this fraction fa and highest ratios of fa/fb1, fa/fb1-2, and fa/fb1-3. Genotype 9 had the lowest percentage of fraction fb1 and highest percentage of fb3. Genotype 6 had the highest fb1, and the lowest fb2 and fb3. Similar trends were observed for the molar-based values. Overall the unit chain length distributions (mean values) of sweetpotato amylopectins were in comparable levels to previous reports on sweetpotato amylopectins (Hanashiro et al., 1996; McPherson & Jane, 1999) with some discrepancies, possibly due to the inclusion of longer chains with DP more than 60 in this study.

Sweetpotato starch usually has a C- or C_a-type X-ray allomorph (Tian et al., 1991). Compared with amylopectins from amaranth starch (Kong et al., 2008) which has a typical A-type polymorph, sweetpotato amylopectins had less of fa, and more of both fb2 and fb3. In comparison to potato starch (McPherson & Jane, 1999), which has a typical B-type polymorph, sweetpotato amylopectins had higher fa, and lower fb2 and fb3. This supported the suggestion that amylopectin molecular structures reflect the structures of their granular starch (Vermeylen et al., 2004).

Some detailed information on the peak-DP of weight-based unit chain length profile of some chain categories and sub-categories of sweetpotato amylopectins from different genotypes are also summarized in Table 2. For the short chains of amylopectins (DP 6–36), several subgroups were noted as illustrated in Fig. 1Bw. This generally agreed with previous observations (McPherson & Jane, 1999). A major peak was observed at DP 13 (DP 12 on a molar basis) for all the sweetpotato amylopectins. There was also a protruding area around DP 19–20, forming a peak or just a shoulder, depending on the genotypes. For example, amylopectin of genotype 6 had a protruding shoulder around DP 19–20 (Fig. 1Bw), whereas that of genotype 8 had an obvious peak at DP 19 instead (Fig. 1Cw). Most sweetpotato amylopectin had their peak position of these protruding shoulders or peaks at DP 19 except genotype 2 had that at DP 20. This profile of short chains corresponded to some cases from group 3 according to the structural division of amylopectins based on the unit chain length distribution of internal chains (Bertoft et al., 2008). Another characteristic subgroup of short chains is from DP 6–8, termed A_{fp}-chain (fingerprint A-chain) (Bertoft, 2004). This A_{fp} profile of sweetpotato amylopectins was different from the other amylopectins from other plants (Bertoft et al., 2008; Jane et al., 1999; Koizumi, Fukuda, & Hizukuri, 1991), but consistent to each other within the amylopectins of different sweetpotato genotypes. Wide genetic variations were also found in the molar amount of A_{fp} from 11.75% in genotype 3–9.40% in genotype 11 with a mean value of 10.8% (Table 3). Compared with amylopectins in other 17 plants from a previous study (Bertoft et al., 2008), molar amounts of A_{fp} in sweetpotato amylopectins were generally higher, with the single exception of Andean yam beans that possessed a very high content (14.1%).

Table 2
Peak-DP of weight-based unit chain length of diverse chain categories and sub-categories of amylopectins from 11 sweetpotato genotypes.[a]

Genotype	Amylopectins				φ,β-Limit dextrins			
	A_{fp}	S_{ap}	Shoulder	L_{ap}	B_{fp}	B_{fp} shoulder	BS_{major}	B2
1	7	13	19	47	7	5	10	33
2	7	13	20	45	7	5	10	33
3	7	13	19	47	7	5	10	33
4	7	13	19	47	7	5	9	32
5	7	13	19	48	7	5	10	34
6	7	13	19	47	7	5	9	33
7	7	13	19	48	7	5	10	35
8	7	13	19	47	7	5	10	34
9	7	13	19	47	7	5	10	34
10	7	13	19	48	7	5	9	34
11	7	13	19	47	7	5	9	34

A_{fp}: fingerprint A-chains of amylopectins; S_{ap}: short chains of amylopectins (DP 6–36); shoulder: protruding areas of short chains of amylopectins; L_{ap}: long chains of amylopectins (DP > 36); B_{fp}: fingerprint B-chains of φ,β-limit dextrins; B_{fp} shoulder: protruding areas of B_{fp}; BS_{major}: chains with DP 8–25 of φ,β-limit dextrins; B2: DP 26–55.

[a] Genotype codes were according to Table 1.

For the long chains of amylopectins (DP > 36), two subgroups (B2 and B3) were noted with peaks DP 45–48 (B2) (Table 2), and peak or shoulder around DP 72 (B3), depending on the specific genotypes (Fig. 1Bw). The subgroup at DP around 72 was not distinguished as a clear peak. It should be noted that chains longer than DP at around 60 were not resolved as individual peaks in HPAEC system (column: CarboPac PA-100). Nevertheless, chain length with DP higher than 60 can be approximately obtained by continuous dividing the chromatogram into corresponding peaks until reaching the baseline (Bertoft, 2004). This was further supported by the application of a CarboPac PA-200 column, which has higher resolution and sensitivity than the commonly used CarboPac PA-100, and could resolve the individual peaks up to around DP 105 in HPAEC system (unpublished data).

3.2. Unit chain length distributions of φ,β-limit dextrins

The external part of chains in amylopectins was sequentially hydrolyzed by phosphorylase *a* and β-amylase to obtain their φ,β-limit dextrins, which provide structural information of the internal part of amylopectins (Bertoft, 1989). By debranching, all the A-chains (Peat et al., 1952) appeared as maltose peak, and the rest were B-chains. The molar amount of A-chains in the form of maltose in φ,β-limit dextrins (Table 3) varied greatly among different genotypes from 54.28% in genotype 7–48.84% in genotype 8 with a mean of 51.74%, lower than that of amaranth (Kong et al., 2008), and amylose-free potato amylopectins (Bertoft, 2004). In general, the wide range of molar amount of A-chains in sweetpotato genotypes was rather comparable to that of 17 other amylopectins reported (Bertoft et al., 2008). From the difference in the amounts of A-chains and A_{fp}-chains, the amount of A_{clsr} (clustered A-chains) can be calculated and also showed wide variations (37.29% in genotype 8–43.59% in genotype 7) between different genotypes, with a mean of 40.94%, lower than most of the other samples previously reported (Bertoft et al., 2008).

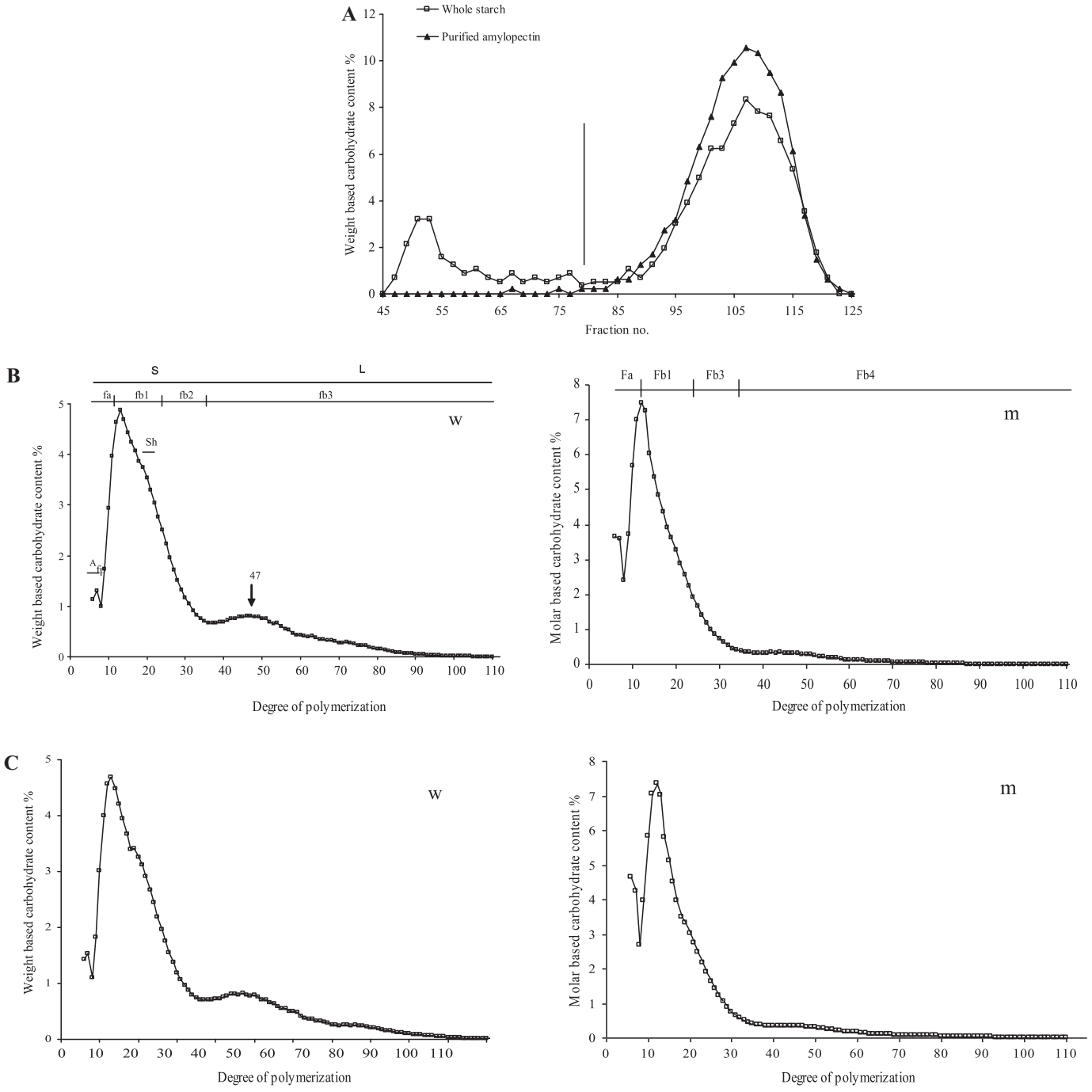

Fig. 1. Chromatograms of sweetpotato amylopectins: (A) Gel permeation chromatograms (Sepharose CL 6B) of debranched whole starch and purified amylopectin from sweetpotato genotype 9; (B and C) HPAEC chromatograms of unit chain length distribution of amylopectins obtained by debranching amylopectins of sweetpotato genotypes 6 (B) and 8 (C), "w" represents weight-based percentages, "m" represents molar-based percentages, "f" denotes weight-based division, "F" denotes molar-based division. The straight line (fraction no. 79) in A denotes the division of amylose and amylopectin fractions. "sh" in the Bw denotes "shoulder". DP ranges for diverse chain categories as in Tables 1–3.

Examples of the internal B-chain distributions from genotypes 6 and 8 are illustrated in Fig. 2, and some of the detailed characteristics on the weight basis are summarized in Table 2. On weight-based distribution, two distinguishable peaks were observed with a clear third peak in some genotypes in the long chains area. Among the short B-chains (DP 3–25), two structural subgroups could be identified (Bertoft, 2004), i.e., the shortest B-chains with DP 3–7 and the majority of short B-chains with DP 8–25 (BS_{major}). In analogy to A_{fp} in whole amylopectins, previously the first group was termed B_{fp} (fingerprint B-chains) because its characteristic profile varied in different samples from different plant species (Bertoft, 2004; Bertoft et al., 2008). However, in this study, two types of profiles of B_{fp} (especially regarding DP 3) were observed in φ,β-limit dextrins of amylopectins of different sweetpotato genotypes (e.g., Fig. 2Aw of genotype 6 in contrast to Fig. 2Bw of genotype 8). For B_{fp} area in the chromatograms on a weight basis (Fig. 2Aw and Fig. 2Bw), a shoulder was observed, and all the genotypes had the same shoulder-position at DP 5 and

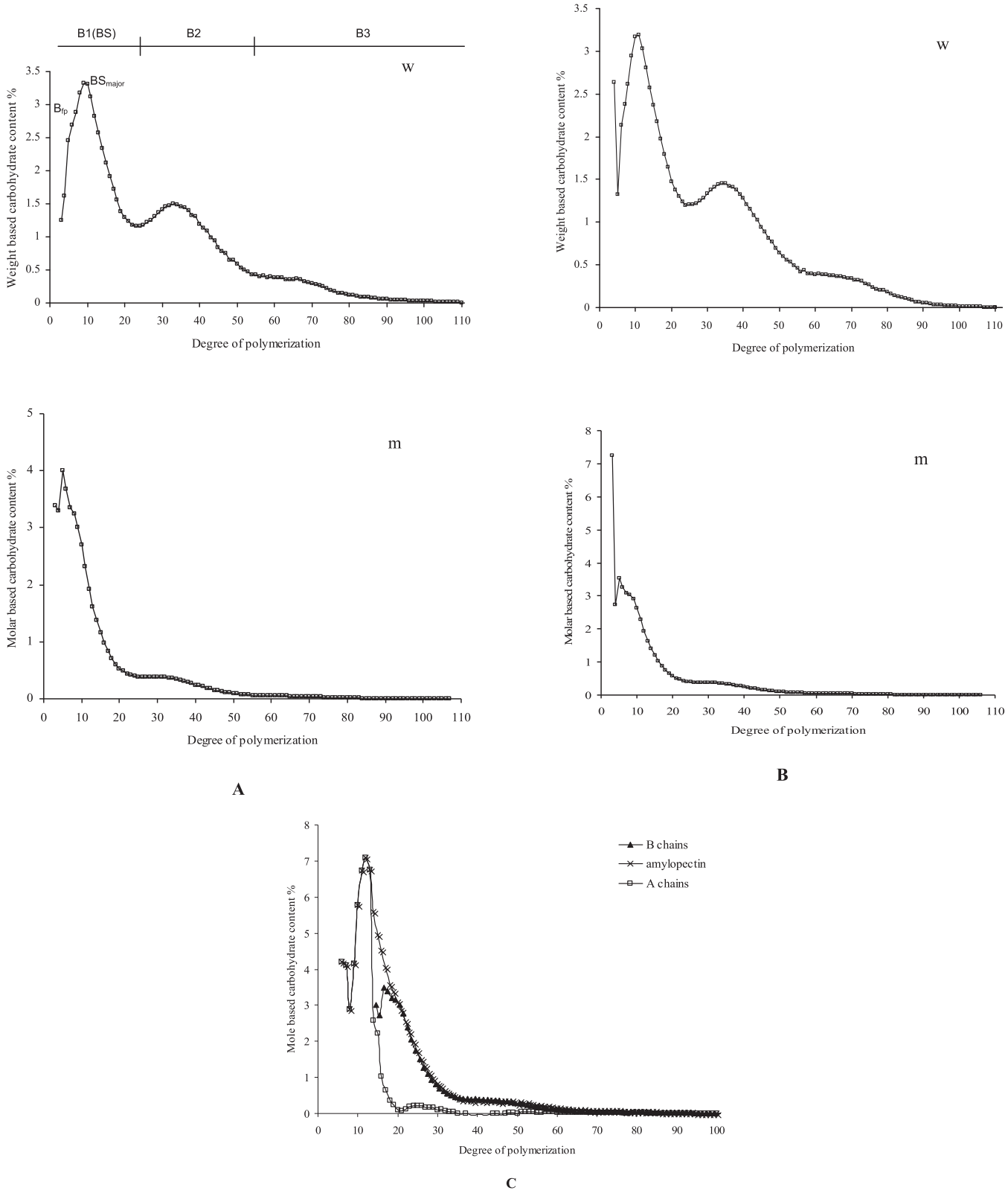

Fig. 2. HPAEC chromatograms of unit chain length distribution of internal B-chains obtained by debranching φ,β-limit dextrins of sweetpotato amylopectins: (A) genotype 6; (B) genotype 8; (C) Comparison in molar-based unit chain length distributions of original amylopectin (genotype 1) with reconstructed amylopectin from their φ,β-limit dextrins assuming that all the individual unit chains had the same external chain length (ECL). "w" represents weight-based percentages, "m" represents molar-based percentages. DP ranges for diverse chain categories as in Table 3.

Table 3
Molar percentage (%) of diverse chain categories in sweetpotato amylopectins and their φ,β-limit dextrins.[a]

Genotype	A_{fp}	A	A_{clsr}	B_{fp}	BS_{major}	B1(BS)	B2	B3	BL	S
1	11.26^{bc}	51.62^{de}	40.36^{de}	15.87^{c}	23.93^{ab}	39.80^{c}	7.41^{a}	1.18^{ab}	8.59^{a}	91.41^{ab}
2	11.21^{bc}	51.81^{cd}	40.60^{de}	15.49^{cd}	24.23^{a}	39.73^{c}	7.31^{a}	1.16^{ab}	8.47^{ab}	91.54^{ab}
3	11.75^{ab}	53.41^{ab}	41.66^{bc}	15.02^{d}	23.48^{bc}	38.50^{d}	7.02^{b}	1.08^{b}	8.10^{b}	91.91^{a}
4	9.96^{cd}	51.40^{de}	41.44^{cd}	16.95^{b}	23.18^{cd}	40.12^{bc}	7.33^{a}	1.16^{ab}	8.49^{ab}	91.52^{ab}
5	11.33^{ab}	53.96^{a}	42.64^{ab}	15.39^{cd}	22.44^{de}	37.82^{e}	7.12^{b}	1.10^{ab}	8.22^{ab}	91.78^{ab}
6	9.66^{d}	51.08^{de}	41.42^{cd}	17.72^{b}	23.08^{cd}	40.80^{b}	7.08^{b}	1.05^{b}	8.13^{b}	91.87^{ab}
7	10.69^{c}	54.28^{a}	43.59^{a}	15.72^{cd}	21.57^{f}	37.28^{e}	7.22^{ab}	1.22^{a}	8.44^{ab}	91.56^{ab}
8	11.55^{ab}	48.84^{f}	37.29^{f}	19.86^{a}	23.08^{cd}	42.95^{a}	7.10^{b}	1.12^{ab}	8.22^{ab}	91.79^{ab}
9	11.26^{bc}	52.70^{bc}	41.44^{cd}	15.40^{cd}	23.28^{bc}	38.68^{d}	7.32^{a}	1.29^{a}	8.62^{a}	91.38^{b}
10	10.96^{bc}	51.26^{ed}	40.30^{de}	17.81^{b}	22.38^{e}	40.19^{bc}	7.38^{a}	1.18^{ab}	8.57^{a}	91.44^{ab}
11	9.40^{d}	49.13^{f}	39.73^{e}	20.25^{a}	22.13^{ef}	42.37^{a}	7.30^{a}	1.21^{a}	8.51^{a}	91.50^{ab}
Mean	10.80	51.74	40.94	16.90	22.97	39.87	7.23	1.15	8.39	91.61

A_{fp}: fingerprint A-chains of amylopectins (DP 6–8); A_{clsr}: A-chains clustered in amylopectins = all A-chains – A_{fp}; B_{fp}: fingerprint B-chains of φ,β-limit dextrins (DP 3–7); BS_{major}: majority of short B-chains in φ,β-limit dextrins = BS – B_{fp} (i.e., DP 8–25), B1 = BS: short B-chains with DP from 3 to 25 in φ,β-limit dextrins, B2: DP 26–55 chains in φ,β-limit dextrins, B3: DP > 56 chains in φ,β-limit dextrins; BL (long B-chains) = B2 + B3 in φ,β-limit dextrins; S (short chains) = A + BS in φ,β-limit dextrins; values in the same column with the different superscript letters differ significantly ($p < 0.05$).

[a] Genotype codes were according to Table 1.

the highest amount of specific chain at DP 7 (Table 2). BS_{major} (DP 8–25) had peak positions at DP 9 or 10, depending on the specific genotypes. This profile was apparently not related to the plant species (Bertoft et al., 2008). For the chromatograms on a molar-basis, B_{fp} chains formed the sharpest peak group with peak position at DP 5, whereas the group of longer B3-chains was hardly distinguishable (Fig. 2Am and Fig. 2Bm). Wide variations were also observed in the molar amounts of B_{fp} (from 15.02% in genotype 3–20.25% in genotype 11 with a mean of 16.9%) and BS_{major} (from 24.23% in genotype 2–21.57% in genotype 7 with a mean of 22.97%) among different genotypes (Table 3). This genetic variation in B_{fp} profiles was also observed in cassava samples (Laohaphatanaleart et al., 2009), indicating B_{fp} area was not as highly conserved as A_{fp} in specific plants in the course of evolution. Compared with other amylopectins, molar amounts of B_{fp} of sweetpotato φ,β-limit dextrins was a little lower than that of amaranth (Kong et al., 2008), and higher than that of diverse amylopectins in group 3 and group 4 (Bertoft et al., 2008), whereas BS_{major} amount was higher than that in group 4 and lower than group 1 and thus was not strictly related to the polymorph type. For molar amounts of all the short chains in the φ,β-limit dextrins (S = A + BS), only smaller variations among different genotypes were observed (from 91.38% in genotype 3–91.91% in genotype 9) (Table 3). Since short chains are likely to participate in structuring clusters (Bertoft, 2004; Bertoft, 2007a), this relatively constant amount of S-chains may indicate a rather similar cluster size in diverse sweetpotato amylopectins.

DP 3 in the φ,β-limit dextrins derives from the shortest possible internal segment (ICL = 1) found in amylopectins (Kainuma & French, 1969), and was suggested to be involved in structuring branched building blocks in amylopectin clusters (Bertoft & Koch, 2000). The difference in the amounts of DP 3 and other short B-chain categories indicated possible difference in the building block organization in different sweetpotato amylopectin genotypes.

For longer B-chains in the φ,β-limit dextrins (DP > 25), two subgroups, B2 (DP 26–55) and B3 (DP > 55), could be clearly observed in weight-based chain length distribution. The peaks of B3 subgroup could hardly be distinguished on molar basis. The peak-position of B2 on a weight basis varied from 32 to 35, depending on the specific genotype (Table 2). This profile fits with the structural features of group 3 and group 4 according to the previous division of internal profiles of amylopectins (Bertoft et al., 2008) as briefed in the Introduction. The general profiles of φ,β-limit dextrins resembled that of their whole amylopectins in terms of the distribution of the peaks, indicating an evenness in their external chain lengths.

Small variations among different genotypes were observed in the molar amounts of B2 and B3 and, thus, BL (B2 + B3) (Table 3). The genetic variations in the amounts of long chains were considerably smaller than those of the short chain categories, indicating longer chains were more conserved during evolution. Compared with amylopectins of group 1 (Bertoft et al., 2008), the proportion of long B-chains of sweetpotato, especially B3 (mean values: 1.15% (B3), 7.23% (B2)), was higher, but lower than that of group 4, which consisted of B-polymorph starches, possibly indicating a difference in the interconnections between the clusters either according to the model of Hizukuri (1986) or Bertoft (2004).

3.3. Chain lengths of diverse chain categories in amylopectins and their φ,β-limit dextrins

Chain lengths of different chain categories in sweetpotato amylopectins and φ,β-limit dextrins were calculated (Table 4). Small variations in CL_{ap} (average chain length of amylopectin) among different genotypes were recorded from 19.92 in genotype 11–19.36 in genotype 6 with a mean of 19.60. Sweetpotato CL_{ap} in this study was generally lower than the results from previous studies on sweetpotato amylopectins (McPherson & Jane, 1999; Takeda, Tokunaga, Takeda, & Hizukuri, 1986), probably due to the different methods employed in different studies. However, direct comparisons could be made between samples with comparable method (Bertoft et al., 2008; Kong et al., 2008; Laohaphatanaleart et al., 2009). Sweetpotato CL_{ap} was generally in comparable levels with some C-type starches, higher than A-type, but lower than B-type starches (Bertoft et al., 2008). This general trend agreed with previous observations using different analytical methods (Hanashiro et al., 1996; Hanashiro, Tagawa, Shibahara, Iwata, & Takeda, 2002; Hizukuri, 1985; Jane et al., 1999). Further details on average unit chain lengths of short (DP 6–36) (SCL_{ap}, mean 16.11) and long (DP > 36) (LCL_{ap}, mean 54.31) chains in amylopectins revealed that sweetpotato roughly had LCL_{ap} higher than that of A-type and lower than B-type starches with the exception of Andean yam bean, without being able to fit into any of the four groups (Bertoft et al., 2008).

Because the internal structures of amylopectins could be critical in the overall starch structure (O'Sullivan & Pérez, 1999), some average chain lengths from the internal part was calculated in the form of φ,β-limit dextrins. Chain length of φ,β-limit dextrins (CL_{ld}, mean 8.30), chain length of B-chains in φ,β-limit dextrins (BCL_{ld},

Table 4
φ,β-Limit value and chain lengths of chain categories in sweetpotato amylopectins and their φ,β-limit dextrins.[a]

Genotype	CL_{ap}	SCL_{ap}	LCL_{ap}	CL_{ld}	BCL_{ld}	BS-CL_{ld}	BL-CL_{ld}	ECL	ICL	TICL	NC:B	φ,β-LV (%)
1	19.53^{b}	16.10^{ab}	54.19^{bc}	8.50^{a}	15.43^{ab}	9.92^{ab}	40.96^{ab}	12.54^{b}	6.00^{a}	14.43^{a}	2.06^{ab}	56.50^{d}
2	19.51^{b}	15.92^{b}	53.88^{c}	8.47^{a}	15.44^{ab}	10.00^{a}	40.90^{b}	12.54^{b}	5.97^{a}	14.44^{a}	2.07^{ab}	56.59^{d}
3	19.63^{ab}	16.08^{ab}	54.50^{b}	8.21^{ab}	15.33^{ab}	10.01^{a}	40.61^{bc}	12.92^{a}	5.71^{b}	14.33^{ab}	2.13^{ab}	58.18^{ab}
4	19.66^{ab}	16.24^{a}	54.11^{bc}	8.35^{ab}	15.05^{ab}	9.64^{ab}	40.65^{bc}	12.81^{ab}	5.85^{ab}	14.05^{b}	2.05^{bc}	57.54^{c}
5	19.37^{b}	16.01^{ab}	54.25^{bc}	8.14^{b}	15.34^{ab}	9.81^{ab}	40.77^{bc}	12.73^{ab}	5.64^{b}	14.34^{ab}	2.16^{a}	57.97^{bc}
6	19.36^{b}	16.20^{ab}	53.49^{c}	8.18^{b}	14.62^{cd}	9.50^{bc}	40.28^{c}	12.68^{ab}	5.68^{b}	13.62^{bc}	2.04^{bc}	57.76^{bc}
7	19.81^{a}	16.18^{ab}	54.70^{b}	8.17^{b}	15.49^{a}	9.68^{ab}	41.15^{ab}	13.14^{a}	5.67^{b}	14.49^{a}	2.17^{a}	58.75^{a}
8	19.40^{b}	15.96^{b}	54.38^{b}	8.26^{ab}	14.23^{d}	9.18^{bc}	40.59^{bc}	12.65^{ab}	5.76^{ab}	13.23^{c}	1.96^{c}	57.45^{c}
9	19.76^{ab}	16.05^{ab}	55.35^{a}	8.44^{a}	15.68^{a}	9.92^{ab}	41.55^{a}	12.82^{ab}	5.95^{a}	14.05^{b}	2.03^{bc}	57.24^{cd}
10	19.59^{ab}	16.07^{ab}	54.74^{b}	8.32^{ab}	14.96^{bc}	9.40^{bc}	41.03^{ab}	12.77^{ab}	5.82^{ab}	13.96^{b}	2.05^{bc}	57.54^{bc}
11	19.92^{a}	16.36^{a}	54.18^{bc}	8.28^{ab}	14.34^{d}	9.02^{c}	40.85^{bc}	13.15^{a}	5.78^{ab}	13.34^{c}	1.97^{c}	58.46^{ab}
Mean	19.60	16.11	54.31	8.30	15.06	9.63	40.82	12.79	5.80	14.02	2.06	57.64

CL_{ap}: average chain length of amylopectin; SCL_{ap}: average chain length of short chains (DP 6–36) of amylopectins; LCL_{ap}: average chain length of short chains (DP > 36) of amylopectins; CL_{ld}: average chain length of φ,β-limit dextrins; BS-CL_{ld}: average chain length of short B-chains (DP 3–25) of φ,β-limit dextrins; BL-CL_{ld}: average chain length of long B-chains (DP > 25) of φ,β-limit dextrins; ECL: average external chain length of amylopectin = $CL_{ap} - CL_{ld} + 1.5$, in which 1.5 is according to action patterns of phosphorylase *a* and β-amylase; ICL: average internal chain length of amylopectin = $CL_{ap} - ECL - 1$, in which 1 represents the branching point; TICL: average total internal chain length of amylopectin = $BCL_{ld} - 1$, in which 1 represents the branching point, BCL_{ld} is the average chain length of B-chains of φ,β-limit dextrins; NC:B: average number of chains per B-chain in φ,β-limit dextrins = TICL/(ICL + 1); φ,β-LV: φ,β-limit value = $100 - 100 \times CL_{ld}/CL_{ap}$; values in the same column with the different superscript letters differ significantly ($p < 0.05$).

[a] Genotype codes were according to Table 1.

mean 15.06), and total internal chain length (TICL, mean 14.06) (Bertoft, 1991) were generally related to the type of polymorph of granular starches (Bertoft et al., 2008). For the B-chains in φ,β-limit dextrins, chain length of short B-chains (DP 3–25) (BS-CL_{ld}, mean 9.63) appeared not to be related to polymorph type whereas chain length of long B-chains (DP > 25) (BL-CL_{ld}, mean 40.82) did. This is consistent with the trends from the whole amylopectins. From the difference in the average unit chain lengths of amylopectins (CL_{ap}) and their φ,β-limit dextrins (CL_{ld}), φ,β-limit value (φ,β-LV, mean 57.64%), average external chain length (ECL, mean 12.79), average internal chain length (ICL, mean 5.80), and number of chains per B-chain (NC:B, mean 2.06) were obtained. Apparently, φ,β-LV and NC:B were not strictly linked to type of polymorph, whereas sweetpotato ECL and ICL fitted with the structural features of C-type polymorph starch in general, and thus fell within the features of group 2 and group 3 (Bertoft et al., 2008).

It was shown that CL_{ap}, ECL and ICL were proportionally linked to each other in diverse samples (Bertoft et al., 2008). In this study, Pearson correlation analysis showed that CL_{ap} was positively correlated with ECL ($r = 0.80$, $p < 0.01$), but little with ICL. Neither was ECL nor ICL related with each other, indicating a possible different branching pattern within the sweetpotato genotypes. Some structural parameters in different starches were directly linked to the type of polymorph of their granules (Bertoft et al., 2008). This trend was not outweighed by the variations in these structural parameters among different sweetpotato genotypes in comparison with other samples (Bertoft et al., 2008; Kong et al., 2008; Laohaphatanaleart et al., 2009). Pearson correlation analysis also revealed that some parameters were linked to each other (high correlation coefficients). For example, ICL was highly correlated with CL_{ld} ($r = 0.99$, $p < 0.001$), and φ,β-LV was highly linked to ECL ($r = 0.88$, $p < 0.001$) and ICL ($r = -0.83$, $p < 0.01$), indicating that they can be interchangeably used to predict each other. Pearson correlation analysis between the chain lengths (Table 4) and molar amounts (Table 3) of diverse chain categories revealed the possible linkages between different structural parameters. E.g., NC:B was highly positively correlated with molar amount of A ($r = 0.94$, $p < 0.001$) and negatively with B1-chains ($r = -0.92$, $p < 0.001$). TICL was highly correlated with molar amount of A ($r = 0.86$, $p < 0.001$) and B_{fp}-chains ($r = -0.93$, $p < 0.001$). CL_{ap} was mainly contributed by B3-chains ($r = 0.74$, $p < 0.01$). These correlation analyses may contribute to the development of limited numbers, but efficient independent variants, in illustrating amylopectin structures.

3.4. Theoretical reconstruction of amylopectins from φ,β-limit dextrins

Similar profiles of unit chain length distributions between amylopectins (Fig. 1B and C) and their φ,β-limit dextrins (Fig. 2A and B) might suggest an evenness of the external chain lengths. Pearson correlation analysis further revealed high correlation coefficients between molar- or weight-based amounts of different chain categories from φ,β-limit dextrins and amylopectins. For example, fb3 was highly correlated to B3 ($r = 0.77$, $p < 0.01$) and BL-CL_{ld} ($r = 0.81$, $p < 0.01$); fb1 and BL-CL_{ld} ($r = -0.67$, $p < 0.05$), as well as fb2 and BS-CL_{ld} ($r = 0.65$, $p < 0.05$) were linked closely.

It was also proposed that all the external segments of B-chains in amylopectins have the same chain length (Inouchi, Glover, & Fuwa, 1987). Based on this assumption, theoretical reconstruction of B-chains of amylopectins from their φ,β-limit dextrins could be tested by adding ECL (an average value) minus one (the glucosidic residue at the non-reducing ends of φ,β-limit dextrins) to the individual B-chain lengths of φ,β-limit dextrins. It was found that reconstruction mode values (Bertoft et al., 2008; Laohaphatanaleart et al., 2009) varied within "−1", "0", and "+1", depending on the specific sweetpotato genotypes. An example of genotype 1, in which the reconstruction mode value was "0", is illustrated in Fig. 2C. It was noted that at DP > 20 the two curves fitted well, indicating that at least B-chains in the form of φ,β-limit dextrins with DP > 20 had the same ECL. B-chains with DP < 20 showed discrepancy between the reconstructed curve and the original one. This difference may be attributed to the A-chains which could also be theoretically deduced by the difference between the reconstructed curve (B-chains) and the original amylopectin curve (A- and B-chains). It appeared that long A-chains, which were previously observed in some amylopectins such as Andean yam bean, amylose-free potato, and tapioca (cassava) (Bertoft et al., 2008), were not observed in any of the sweetpotato amylopectins. However, it should be noted that the exact locations of A-chains and some shorter B-chains remain unclear due to the possible overlapping in their chain lengths (Bertoft et al., 2008).

3.5. Molar ratios of selected chain categories in amylopectins and their φ,β-limit dextrins

The molar ratio of A- to B-chains (A:B) can reflect the proportion of Staudinger (Staudinger & Husemann, 1937) and Haworth (Haworth, Hirst, & Isherwood, 1937) conformations in chain inter-

Table 5
Selected molar ratios of diverse chain categories from amylopectins and their φ,β-limit dextrins.[a]

Genotype	A:B	S_{ap}:L_{ap}	BS:BL	A_{clsr}:BS	A_{clsr}:B	B_{fp}:BS_{major}
1	1.07	10.12	4.64	1.01	0.83	0.67
2	1.08	10.17	4.70	1.02	0.84	0.64
3	1.15	9.81	4.77	1.08	0.89	0.64
4	1.06	10.11	4.73	1.03	0.85	0.74
5	1.17	10.39	4.60	1.13	0.93	0.69
6	1.04	10.81	5.02	1.02	0.85	0.77
7	1.19	9.61	4.42	1.17	0.95	0.73
8	0.96	10.17	5.23	0.87	0.73	0.86
9	1.11	9.59	4.49	1.07	0.88	0.66
10	1.05	9.99	4.70	1.00	0.83	0.80
11	0.97	9.63	4.98	0.94	0.78	0.92
Mean	1.08	10.05	4.76	1.03	0.85	0.74

[a] Genotype codes were according to Table 1; diverse chain categories were according to Tables 2–5.

connections in amylopectin, and is best obtained by analyzing the debranched φ,β-limit dextrins (Bertoft, 2004). A:B varied from 0.96 in genotype 8–1.19 in genotype 7 with a mean of 1.08, indicating a similar portion of Staudinger and Haworth conformations in sweetpotato amylopectins. This was generally similar to the amylopectins from other plants (Bertoft et al., 2008; Kong et al., 2008). Different ratios of molar amounts of diverse chain categories have been previously used to tentatively classify diverse amylopectins to four different groups (1–4), mostly based on their internal structural features (Bertoft et al., 2008). Here the ratios from sweetpotato amylopectins were calculated (Table 5) to further test this classification method. S_{ap}:L_{ap} (short chains to long chains in amylopectin) varied from 9.63 in genotype 11–10.81 in genotype 6, making sweetpotato belong to group 3. However, BS:BL varied from 4.42 to 5.23 with a mean of 4.76, generally fitting in group 2. The other ratio parameters hardly fitted within one specific group, or the genetic variations outweighed the proposed structural boundaries between different groups. For example, A_{clsr}:BS ranged from 0.87 to 1.17 with a mean of 1.03; A_{clsr}:B ranged from 0.73 to 0.95 with a mean of 0.85; B_{fp}:BS_{major} ranged from 0.64 to 0.92 with a mean of 0.74. Thus new boundaries should be proposed for new classifications as more types of amylopectins are to be structurally characterized.

Clusters were suggested to be a basic structural unit of amylopectin (Nikuni, 1969; French, 1972). Some ratios (Table 5) may suggest certain possible roles of diverse chain categories in structuring different types of clusters in amylopectin (Bertoft, 2004). For example, assuming that long chains interconnected clusters and short chains formed clusters, then the ratio S_{ap}:L_{ap} (mean 10.5) would closely reflect the number of chains per cluster in amylopectin. This is considerably lower than a previously suggested situation (22–25) (Hizukuri, 1986), but in the similar order with experimental values obtained by α-amylolysis method (Bertoft, 2007b; Kong, Corke, & Bertoft, 2009). The ratio BL:BS (mean 4.76) might reflect the number of B-chains (BS) forming the clusters in relation to the number of B-chains (BL) interconnecting the clusters. Other alternatives may be: assuming that one A-chain and one B-chain formed a double helix to crystallize in granules (Imberty & Pérez, 1989), and A_{clsr} were these A-chains, thus A_{clsr}:B (mean 0.85) would be 1 if assuming that all the B-chains participated in double helix formation (Laohaphatanaleart, Piyachomkwan, Sriroth, & Bertoft, 2010), whereas A_{clsr}:BS (mean 1.03) would be 1 when assuming that only the short B-chains participated in double helix formation (Bertoft, 2004). Some features of the structural organization of building blocks in clusters (Bertoft, 2007b) may also be reflected by B_{fp}:BS_{major} (mean 0.74), as B_{fp} may be interconnected by BS_{major} to form large building blocks.

Nevertheless, these ratios in relation to the actual amylopectin structure remain assumptional until structural definition of a cluster in the amylopectin could be experimentally clarified. Furthermore, genetic variations in different sweetpotato genotypes may contribute uncertainty in the exact structural boundary in distinguishing the functional roles of different chain categories.

3.6. Amylopectin molecular structures in relation to thermal and pasting properties of granular starch

Several physical properties of sweetpotato starches, including gelatinization (onset temperature: T_o, peak temperature: T_p, conclusion temperature: T_c, gelatinization temperature range: ΔT, and gelatinization enthalpy: ΔH) and pasting properties (peak viscosity: PV, hot paste viscosity: HPV, breakdown viscosity: BD, cold paste viscosity CPV, setback viscosity: SB, and peak time: P_{time}) are given in supplementary materials (Table S1). Pearson correlation analysis revealed that certain structural features of amylopectins may be critical to some physical properties of sweetpotato starch (Table 6).

For the fractions from amylopectins, T_p and T_c were negatively correlated to fa ($r = -0.88$, $p < 0.001$ and $r = -0.86$, $p < 0.001$) and fb2 ($r = -0.71$, $p < 0.05$ and $r = -0.78$, $p < 0.01$), but positively correlated to fb1 ($r = 0.75$, $p < 0.01$ and $r = 0.82$, $p < 0.01$). This generally agreed with previous studies on different types of starch (Kong et al., 2008; Koroteeva et al., 2007; Noda et al., 1998; Okuda, Aramaki, Koseki, Satoh, & Hashizume, 2005; Patinol & Wang, 2003). A possible explanation may be that fa-chains would cause structural defects in the crystals of the granules, which may be built up by chains mainly from fb1 (Genkina et al., 2007). Further detailed analysis showed that A_{fp} (a fraction of fa) was negatively and strongly correlated to T_p ($r = -0.94$, $p < 0.001$) and T_c ($r = -0.97$, $p < 0.001$), indicating these chains of DP 6–8 actually form the defects in the crystallites (Genkina et al., 2007; Kozlov et al., 2007) since they may be too short to form double helices (Gidley & Bulpin, 1987). In contrast, A_{clsr} was positively related to T_o ($r = 0.82$, $p < 0.01$), and ΔH ($r = 0.69$, $p < 0.05$), and negatively with ΔT ($r = -0.68$, $p < 0.05$), indicating these chains may indeed form the clusters that crystallized in the granules (Bertoft, 2004). The longer chains (e.g., fb2) may serve as the backbones which would more facilitate the gelatinization as proposed in a side-chain liquid-crystalline model for starch (Waigh et al., 2000). It should also be noted that fa (Hanashiro et al., 1996) and A-chains (Bertoft, 2004) had different correlationships with physical properties, thus they should refer to different parts of the amylopectins, and is consistent with the reconstruction results as discussed in Section 3.4 that A-chains not only covered a broader DP range than fa, but also represented considerable more chains by number. Previous studies showed that CL_{ap} correlated well with thermal properties of diverse types of starches (Jane et al., 1999; Kong et al., 2008; Okuda et al., 2005; Stevenson, Yoo, Hurst, & Jane, 2005). In this study, little correlation was found between CL_{ap} and thermal properties of sweetpotato starch, possibly due to the small variations in CL_{ap} among different genotypes (Table 4).

It was proposed that the amorphous part of granular starch (mostly internal part of amylopectin) may be critical in the gelatinization behaviors of starches (Donovan, 1979; Genkina et al., 2007; Slade & Levine, 1988; Waigh et al., 2000), and was previously supported by data from amaranth starches (Kong et al., 2008). Indeed, some parameters on the internal part of the amylopectins showed correlations with the gelatinization and pasting features of sweetpotato starches (Table 6). For example, B_{fp} was negatively correlated with ΔH ($r = -0.73$, $p < 0.05$), and positively with ΔT ($r = 0.80$, $p < 0.01$). This may be explained by the starch side-chain liquid-crystalline model (Waigh et al., 2000) that B_{fp} may contribute to the composition of the flexible "spacers", and higher amount of B_{fp}-chains would contribute with more flexible

Table 6
Pearson correlation coefficients between molecular structural and physical parameters.[a]

	fa	fb1	fb2	fb3	CL_{ap}	SCL	LCL	A	A_{fp}	A_{clsr}	B_{fp}	BS_{major}	B1(BS)	B2	B3	BL	S:A + BS	ECL	ICL	TICL	NC:B	BCL_{id}
PV	0.61*	−0.56	0.67*	0.12	−0.27	−0.48	0.28	0.65*	0.67*	0.37	−0.81**	0.42	−0.66*	0.10	0.02	0.08	−0.23	−0.42	0.30	0.77**	0.56	0.78**
HPV	0.40	−0.53	0.75**	0.18	−0.08	−0.25	0.24	0.49	0.57	0.26	−0.67*	0.44	−0.51	0.10	0.07	0.09	−0.29	−0.27	0.34	0.65*	0.42	0.65*
BD	0.69*	−0.48	0.48	0.03	−0.39	−0.60	0.27	0.67	0.64*	0.41	−0.79**	0.34	−0.68*	0.08	−0.03	0.05	−0.13	−0.48	0.21	0.75**	0.60	0.75**
CPV	0.50	−0.50	0.67*	0.12	−0.20	−0.34	0.26	0.45	0.59	0.20	−0.62*	0.42	−0.47	0.10	0.06	0.09	−0.24	−0.37	0.33	0.59	0.38	0.61*
SB	0.48	−0.03	−0.11	−0.18	−0.45	−0.40	0.12	0.00	0.25	−0.12	−0.02	0.03	−0.01	0.06	−0.03	0.04	0.12	−0.44	0.06	−0.00	−0.03	0.03
P_{time}	−0.83**	0.77**	−0.56	−0.56	0.31	0.84***	−0.54	−0.57	−0.91***	−0.17	0.61*	−0.15	0.57	0.07	−0.09	0.01	0.08	0.33	−0.08	−0.55	−0.50	−0.61*
T_o	−0.48	0.17	−0.16	0.07	0.39	0.51	0.05	0.59	−0.36	0.82**	−0.41	−0.33	−0.58	−0.19	−0.03	−0.14	−0.03	0.58	−0.39	0.35	0.55	0.35
T_p	−0.88***	0.75**	−0.71*	−0.23	0.40	0.83**	−0.39	−0.44	−0.94***	−0.02	0.60	−0.40	0.44	−0.02	−0.02	−0.03	0.13	0.53	−0.29	−0.56	−0.39	−0.58
T_c	−0.86***	0.82**	−0.78**	−0.32	0.33	0.87***	−0.39	0.39	−0.97***	0.05	0.55	−0.40	0.40	0.02	−0.02	−0.00	0.14	0.46	−0.27	−0.54	−0.37	−0.54
ΔT	−0.28	0.41	−0.60*	−0.12	0.05	0.21	−0.04	−0.83**	−0.44	−0.68*	0.80**	−0.10	0.80**	0.38	0.28	0.38	−0.10	−0.11	0.27	−0.79**	−0.89***	−0.65*
ΔH	0.15	−0.20	0.32	0.01	−0.00	−0.09	0.04	0.70*	0.14	0.69*	−0.73*	0.07	−0.74**	0.40	0.18	0.34	−0.34	−0.13	0.21	0.86***	0.70*	0.77**

* Correlation is significant at $p < 0.05$ level.
** Correlation is significant at $p < 0.01$ level.
*** Correlation is significant at $p < 0.001$ level.
[a] Genotype codes were according to Table 1; Different chain categories and fractions were according to Tables 3–5, and S1.

"spacers". TICL was positively related to ΔH ($r = 0.86$, $p < 0.001$), and negatively with ΔT ($r = -0.79$, $p < 0.01$), resembling the trend from CL_{ap} in previous reports (Kong et al., 2008; Okuda et al., 2005). This may suggest evenness in the external segments of chains as discussed above.

A previous study on the amaranth starch showed that some other parameters (e.g., B3) from φ,β-limit dextrins were related to the physical properties (Kong et al., 2008). However, in this study internal structural parameters such as B2, B3, BL, S (A + BS), and ICL did not show correlations with physical properties, possibly due to the limited variations in the structural values among different genotypes (Tables 3–4). Another possible explanation may be the overlapping of chains with the same length but different functional roles (e.g., as spacer or backbone (Waigh et al., 2000) in amylopectin architecture, which might not be distinguished by debranching in this study.

Pasting properties were also related to some of the amylopectin structural parameters. Fractions fa and fb2 gave higher viscosities to the paste. For example, fa and fb2 positively correlated with PV ($r = 0.61$, $p < 0.05$ and $r = 0.67$, $p < 0.01$). fa and fb2 were negatively ($r = -0.83$, $p < 0.01$) and positively ($r = 0.77$, $p < 0.01$) correlated with P_{time}, respectively. This agreed with previous reports on sweetpotato starch (Takahata et al., 2010). Some of fa may cause structural defects (e.g., A_{fp} contributed greater effects in the higher peak viscosity ($r = 0.67$, $p < 0.05$) and shorter P_{time} ($r = -0.91$, $p < 0.001$)) in the crystallites (formed mainly by fb1-chains) in granules so that water molecules may more easily penetrate into the granules and facilitate their swelling and disintegration (Kozlov et al., 2007; Noda et al., 2009) during heating and shearing, whereas fb2 may serve as backbones in side-chain liquid-crystalline model for starch as discussed above (Waigh et al., 2000). Internal structural parameters also showed their influence on the pasting of starches. For example, PV was positively correlated with TICL ($r = 0.77$, $p < 0.01$) and negatively with B_{fp} ($r = -0.81$, $p < 0.01$), generally supporting the previous proposals that the amorphous part may be important to the physical behaviors of starch (Donovan, 1979; Genkina et al., 2007; Slade & Levine, 1988; Waigh et al., 2000).

This is a complex system and could be reflected in some contradictory results from previous reports. Wider genetic variations are needed to specifically reveal the functional role of diverse chain categories in physical properties. Other components present in the starch granules, such as amylose, phosphorus, proteins, and lipids (Han, Campanella, Guan, Keeling, & Hamaker, 2002; Jane et al., 1999; Tester & Morrison, 1990) or the size distributions and the degree of intact granules (Gujska, Reinhard, & Khan, 1994; Singh, Singh, Isono, & Noda, 2010) may also be influential to the physical properties of granular starch.

4. Conclusions

Wide variations in diverse structural parameters of amylopectins and their φ,β-limit dextrins were observed among 11 different Chinese sweetpotato genotypes. Although the internal structural features of sweetpotato amylopectins partially showed intermediate patterns of group 2 and group 3, where other C-type starches were found, they could not be exactly fitted into any of the 4 groups previously proposed on the basis of internal structure of amylopectins (Bertoft et al., 2008). The group boundaries were further blurred by the genetic variation in these structural parameters, indicating more samples should be analyzed to re-establish new divisions. B_{fp} profiles were not consistent among different sweetpotato genotypes but A_{fp} were, indicating B_{fp} could not be used to fingerprint the plant species from which the starch derived but A_{fp} could. On weight-basis, shoulders with peaks at DP 19–20 for amylopectins and DP 5 for B_{fp} for φ,β-limit dextrins were observed. Pearson correlation analysis revealed that some molecular struc-

tural parameters of the whole amylopectin and their internal part were significantly related to the thermal and pasting properties of granular starches. This study may stimulate further interests on the internal structures of amylopectins and their relationship to the physical properties of starch, to be able to more precisely tailor the starches for diverse food and non-food uses.

Acknowledgements

Sweetpotato roots were kindly provided by associate professor Xinsun Yang at Institute of Crop Science, Hubei Academy of Agricultural Sciences, Wuhan, China. Kind advice from professor Per Åman, Dr. Kristine Koch, and Dr. Roger Andersson at the Department of Food Science, Swedish University of Agricultural Sciences, Uppsala, Sweden, is greatly acknowledged. This research was supported by The University of Hong Kong Seed Funding for Basic Research and The University of Hong Kong Committee on Research and Conference Grants.

Appendix A. Supplementary data

Supplementary data associated with this article can be found, in the online version, at doi:10.1016/j.carbpol.2010.12.039.

References

Bertoft, E. (1989). Partial characterization of amylopectin alpha-dextrins. *Carbohydrate Research*, *189*, 181–193.
Bertoft, E. (1991). Investigation of the fine structure of alpha-dextrins derived from amylopectin and their relation to the structure of waxy-maize starch. *Carbohydrate Research*, *212*, 229–244.
Bertoft, E. (2004). On the nature of categories of chains in amylopectin and their connection to the super helix model. *Carbohydrate Polymers*, *57*, 211–224.
Bertoft, E. (2007a). Composition of clusters and their arrangement in potato amylopectin. *Carbohydrate Polymers*, *68*, 433–446.
Bertoft, E. (2007b). Composition of building blocks in clusters from potato amylopectin. *Carbohydrate Polymers*, *70*, 123–136.
Bertoft, E., & Koch, K. (2000). Composition of chains in waxy-rice starch and its structural units. *Carbohydrate Polymers*, *41*, 121–132.
Bertoft, E., Piyachomkwan, K., Chatakanonda, P., & Sriroth, K. (2008). Internal unit chain composition in amylopectins. *Carbohydrate Polymers*, *74*, 527–543.
Bertoft, E., & Spoof, L. (1989). Fractional precipitation of amylopectin alpha-dextrins using methanol. *Carbohydrate Research*, *189*, 169–180.
Buléon, A., Colonna, P., Planchot, V., & Ball, S. (1998). Starch granules: structure and biosynthesis. *International Journal of Biological Macromolecules*, *23*, 85–112.
Collado, L. S., Mabesa, R. C., & Corke, H. (1999). Genetic variation in the physical properties of sweet potato starch. *Journal of Agricultural and Food Chemistry*, *47*, 4195–4201.
Donovan, J. W. (1979). Phase transitions of the starch-water system. *Biopolymers*, *18*, 263–275.
Dubois, M., Gilles, K. A., Hamilton, J. K., Rebers, P. A., & Smith, F. (1956). Colorimetric method for determination of sugars and related substances. *Analytical Chemistry*, *28*, 350–356.
French, D. (1972). Fine structure of starch and its relationship to the organization of starch granules. *Journal of Japanese Society of Starch Science*, *19*, 8–25.
Genkina, N. K., Wikman, J., Bertoft, E., & Yuryev, V. P. (2007). Effects of structural imperfection on gelatinization characteristics of amylopectin starches with A- and B-type crystallinity. *Biomacromolecules*, *8*, 2329–2335.
Gidley, M. J., & Bulpin, P. V. (1987). Crystallisation of maltooligosaccharides as models of the crystalline forms of starch: Minimum chain-length requirement for the formation of double helices. *Carbohydrate Research*, *161*, 291–300.
Gujska, E., Reinhard, W. D., & Khan, K. (1994). Physicochemical properties of field pea, pinto and navy bean starches. *Journal of Food Science*, *59*, 634–636.
Han, X. Z., Campanella, O. H., Guan, H. P., Keeling, P. L., & Hamaker, B. R. (2002). Influence of maize starch granule-associated protein on the rheological properties of starch pastes. Part II. Dynamic measurements of viscoelastic properties of starch pastes. *Carbohydrate Polymers*, *49*, 323–330.
Hanashiro, I., Abe, J. I., & Hizukuri, S. (1996). A periodic distribution of chain length of amylopectin as revealed by high-performance anion-exchange chromatography. *Carbohydrate Research*, *283*, 151–159.
Hanashiro, I., Tagawa, M., Shibahara, S., Iwata, K., & Takeda, Y. (2002). Examination of molar-based distribution of A, B and C chains of amylopectin by fluorescent labeling with 2-aminopyridine. *Carbohydrate Research*, *337*, 1211–1215.
Haworth, W. N., Hirst, E. L., & Isherwood, F. A. (1937). Polysaccharides. Part XXIII. Determination of the chain length of glycogen. *Journal of the Chemical Society, Chemical Communications*, 577–581.
Hizukuri, S. (1985). Relationship between the distribution of the chain length of amylopectin and the crystalline structure of starch granules. *Carbohydrate Research*, *141*, 295–306.
Hizukuri, S. (1986). Polymodal distribution of the chain lengths of amylopectins, and its significance. *Carbohydrate Research*, *147*, 342–347.
Imberty, A., & Pérez, S. (1989). Conformational-analysis and molecular modeling of the branching point of amylopectins. *International Journal of Biological Macromolecules*, *11*, 177–185.
Inouchi, N., Glover, D. V., & Fuwa, H. (1987). Chain length distribution of amylopectins of several single mutants and the normal counterpart, and sugary-1 phytoglycogen in maize (*Zea mays* L.). *Starch-Stärke*, *39*, 259–266.
International Potato Center (2010). http://www.cipotato.org/sweetpotato/ Accessed 16.11.10.
Jane, J., Chen, Y. Y., Lee, L. F., McPherson, A. E., Wong, K. S., Radosavljevic, M., et al. (1999). Effects of amylopectin branch chain length and amylose content on the gelatinization and pasting properties of starch. *Cereal Chemistry*, *76*, 629–637.
Kainuma, K., & French, D. (1969). Action of pancreatic amylase on starch oligosaccharides containing single glucose side chains. *FEBS Letters*, *5*, 257–261.
Klucinec, J. D., & Thompson, D. B. (1998). Fractionation of high-amylose maize starches by differential alcohol precipitation and chromatography of the fractions. *Cereal Chemistry*, *75*, 887–896.
Koch, K., Andersson, R., & Åman, P. (1998). Quantitative analysis of amylopectin unit chains by means of high-performance anion-exchange chromatography with pulsed amperometric detection. *Journal of Chromatography A*, *800*, 199–206.
Koizumi, K., Fukuda, M., & Hizukuri, S. (1991). Estimation of the distributions of chain length of amylopectins by high-performance liquid chromatography with pulsed amperometric detection. *Journal of Chromatography*, *585*, 233–238.
Kong, X. L., Bertoft, E., Bao, J. S., & Corke, H. (2008). Molecular structure of amylopectin from amaranth starch and its effect on physicochemical properties. *International Journal of Biological Macromolecules*, *43*, 377–382.
Kong, X. L., Corke, H., & Bertoft, E. (2009). Fine structure characterization of amylopectins from grain amaranth starch. *Carbohydrate Research*, *344*, 1701–1708.
Koroteeva, D. A., Kiseleva, V. I., Sriroth, K., Piyachomkwan, K., Bertoft, E., Yuryev, P. V., et al. (2007). Structural and thermodynamic properties of rice starches with different genetic background: Part 1. Differentiation of amylopectin and amylose defects. *International Journal of Biological Macromolecules*, *41*, 391–403.
Kozlov, S. S., Krivandin, A. V., Shatalova, O. V., Noda, T., Bertoft, E., Fornal, J., et al. (2007). Structure of starches extracted from near-isogenic wheat lines—Part II. Molecular organization of amylopectin clusters. *Journal of Thermal Analysis and Calorimetry*, *87*, 575–584.
Laohaphatanaleart, K., Piyachomkwan, K., Sriroth, K., & Bertoft, E. (2010). The fine structure of cassava starch amylopectin. Part 1: Organization of clusters. *International Journal of Biological Macromolecules*, *47*, 317–324.
Laohaphatanaleart, K., Piyachomkwan, K., Sriroth, K., Santisopasri, V., & Bertoft, E. (2009). A study of the internal structure in cassava and rice amylopectin. *Starch-Stärke*, *61*, 557–569.
McPherson, A. E., & Jane, J. (1999). Comparison of waxy potato with other root and tuber starches. *Carbohydrate Polymers*, *40*, 57–70.
Nikuni, Z. (1969). Starch with cooking. *Chori Kagaku*, *2*, 6–14.
Noda, T., Isono, N., Krivandin, A. V., Shatalova, O. V., Blaszczak, W., & Yuryev, V. P. (2009). Origin of defects in assembled supramolecular structures of sweet potato starches with different amylopectin chain-length distribution. *Carbohydrate Polymers*, *76*, 400–409.
Noda, T., Takahata, Y., Sato, T., Suda, I., Morishita, T., Ishiguro, K., et al. (1998). Relationships between chain length distribution of amylopectin and gelatinization properties within the same botanical origin for sweet potato and buckwheat. *Carbohydrate Polymers*, *37*, 153–158.
O'Sullivan, A. C., & Pérez, S. (1999). The relationship between internal chain length of amylopectin and crystallinity in starch. *Biopolymers*, *50*, 381–390.
Okuda, M., Aramaki, I., Koseki, T., Satoh, H., & Hashizume, K. (2005). Structural characteristics, properties, and in vitro digestibility of rice. *Cereal Chemistry*, *82*, 361–368.
Patinol, J., & Wang, Y. J. (2003). Fine structures and physicochemical properties of starches from chalky and translucent rice kernels. *Journal of Agricultural and Food Chemistry*, *51*, 2777–2784.
Peat, S., Whelan, W. J., & Thomas, G. J. (1952). Evidence of multiple branching in waxy maize starch. *Journal of the Chemical Society, Chemical Communications*, 4546–4548.
Pérez, S., & Bertoft, E. (2010). The molecular structures of starch components and their contribution to the architecture of starch granules: A comprehensive review. *Starch-Stärke*, *62*, 389–420.
Sanderson, J. S., Daniels, R. D., Donald, A. M., Blennow, A., & Engelsen, S. B. (2006). Exploratory SAXS and HPAEC-PAD studies of starches from diverse plant genotypes. *Carbohydrate Polymers*, *64*, 433–443.
Singh, S., Singh, N., Isono, N., & Noda, T. (2010). Relationship of granule size distribution and amylopectin structure with pasting, thermal, and retrogradation properties in wheat starch. *Journal of Agricultural and Food Chemistry*, *58*, 1180–1188.
Slade, L., & Levine, H. (1988). Non-equilibrium melting of native granular starch: Part I. Temperature location of the glass-transition associated with gelatinization of A-type cereal starches. *Carbohydrate Polymers*, *8*, 183–208.
Staudinger, H., & Husemann, E. (1937). Über hochpolymere Verbindungen. 150. Mitteilung. Über die Konstitution der Stärke. *Liebigs Annalen der Chemie*, *527*, 195–236.

Stevenson, D. G., Yoo, S. H., Hurst, P. L., & Jane, J. L. (2005). Structural and physicochemical characteristics of winter squash (*Cucurbita maxima* D.) fruit starches at harvest. *Carbohydrate Polymers*, *59*, 153–163.

Takahata, Y., Tanaka, M., Otani, M., Katayama, K., Kitahara, K., Nakayachi, O., et al. (2010). Inhibition of the expression of the starch synthase II gene leads to lower pasting temperature in sweetpotato starch. *Plant Cell Reports*, *29*, 535–543.

Takeda, Y., Tokunaga, N., Takeda, C., & Hizukuri, S. (1986). Physicochemical properties of sweet potato starches. *Starch-Stärke*, *38*, 345–350.

Tester, R. F., & Morrison, W. R. (1990). Swelling and gelatinization of cereal starches. 1. Effects of amylopectin, amylose, and lipids. *Cereal Chemistry*, *67*, 551–557.

Tian, S. J., Rickard, J. E., & Blanshard, J. M. V. (1991). Physicochemical properties of sweet potato starch. *Journal of the Science of Food and Agriculture*, *57*, 459–491.

Vermeylen, R., Goderis, B., Reynaers, H., & Delcour, J. A. (2004). Amylopectin molecular structure reflected in macromolecular organization of granular starch. *Biomacromolecules*, *5*, 1775–1786.

Waigh, T. A., Kato, K. L., Donald, A. M., Gidley, M. J., Clarke, C. J., & Riekel, C. (2000). Side-chain liquid-crystalline model for starch. *Starch-Stärke*, *52*, 450–460.

Zhang, D., Ghislain, M., Huamán, Z., Golmirzaie, A., & Hijmans, R. (1998). RAPD variation in sweetpotato (*Ipomoea batatas* (L.) Lam) cultivars from South America and Papua New Guinea. *Genetic Resources and Crop Evolution*, *45*, 271–277.

Zhang, Z. T. (2001). *Nutritional quality and starch physicochemical properties in sweetpotato (PhD thesis)*. Hong Kong, China: The University of Hong Kong.

Zhu, F., Cai, Y. Z., Yang, X. Y., Ke, J., & Corke, H. (2010). Anthocyanins, hydroxycinnamic acid derivatives, and antioxidant activity in roots of different Chinese purple-fleshed sweetpotato genotypes. *Journal of Agricultural and Food Chemistry*, *58*, 7588–7596.